International Journal of Chemical, Materials and Biomolecular Sciences
ISSN: 2415-6620
Vol:6, No:6, 2012

Role of Viscosity Ratio in Liquid-Liquid Jets under Radial Electric Field

Siddharth Gadkari and Rochish Thaokar

***Abstract*—**The effect of viscosity ratio (λ, defined as viscosity of surrounding medium/viscosity of fluid jet) on stability of axisymmetric (m=0) and asymmetric (m=1) modes of perturbation on a liquid-liquid jet in presence of radial electric field (E_0), is studied using linear stability analysis. The viscosity ratio is shown to have a damping effect on both the modes of perturbation. However the effect was found more pronounced for the m=1 mode as compared to m=1 mode. Investigating the effect of both E_0 and λ simultaneously, an operating diagram is generated, which clearly shows the regions of dominance of the two modes for a range of electric field and viscosity ratio values.

***Keywords*—**liquid-liquid jet, axisymmetric perturbation, asymmetric perturbation, radial electric field

I. Introduction

ELECTRIFIED liquid jets or threads have been widely studied in fluid mechanics. However the same cannot be said about immersed liquid jets, where a jet of liquid is submerged in another immiscible liquid of finite viscosity. In such a case, the viscosity ratio of the jet and the medium fluid ($\lambda = \mu_{medium}/\mu_{jet}$) plays an important role in determining the stability of the system. Also, systems involving immersed jets when subjected to electric fields are now attracting increasing attention. An important occurrence is the electrodispersion of a conducting liquid jet submerged in an immiscible dielectric liquid and subjected to electric field [1]–[3]. A steady "cone- jet" can be realized for a range of system parameters, which can undergo axisymmetric or asymmetric instabilities [4]–[7]. The technique is now used to generate emulsions with narrow distributions of droplet sizes controllable in the range from micrometers to tens of nanometers [4], [8].

There is extensive literature available on both experimental and theoretical investigation of liquid jet breakup, with or without the presence of electric field and several review articles have discussed the topic in ample detail [9]–[11]. Although considerable work has been done on the effect of electric field on jet instabilities, the effect of surrounding medium has not been adequately addressed. The studies in the literature for a jet under radial electric field have either considered the inviscid jet limit ($\lambda = \infty$) [12]–[14] or looked at a viscous jet ($\lambda = 0$) in an inviscid medium [15]–[25].

Siddharth Gadkari is a Phd student of the IITB-Monash Research Academy, IIT Bombay, Mumbai 400076 India (phone: +91-9769066819; e-mail: sidgadkari@iitb.ac.in).

Rochish Thaokar is Associate Professor at Department of Chemical Engineering, IIT Bombay, Mumbai 400076 India (phone: +91 (22) 2576 7241; email: rochish@che.iitb.ac.in

There are few studies which have explicitly considered viscosity of both jet and surrounding, however, limit their discussion to particular values of viscosity ratio [26]–[31] and have not considered the effect of arbitrary viscosity ratio on the different modes of perturbations.

In the present work, we consider a charged liquid jet issuing into another immiscible liquid and subjected to radial electric field. Relative motion between the two fluids is considered zero. We concentrate on the case of high Ohnesorge number (Oh; a dimensionless parameter representing the ratio of viscous and interfacial tension forces), and use linear stability analysis to study the effect of viscosity ratio on the axisymmetric and asymmetric instability of a viscous jet (a perfect conductor) submerged in another viscous fluid (perfect dielectric) subjected to radial electric field. The high Oh limit which has been assumed in this work can be easily satisfied for highly viscous electrified jets. Also it is valid in the study of stability of neutrally buoyant liquid bridges immersed in an outer bath of another immiscible liquid in the presence of electric field [32]–[34]. This type of flow is also encountered in polymer phase separation, where liquid droplets of one of the phases nucleate out and grow and are stretched in extensional flows. Phase separation & morphology under electric field would then depend upon the stability of such threads [35]. The theory developed in the current work, can thus be useful to study all the above interesting systems.

II. Formulation of the Problem

Consider an infinitely long cylindrical jet of radius a of an incompressible liquid with viscosity μ_i, immersed in an immiscible fluid of viscosity μ_e. The subscript i denotes inside fluid jet whereas subscript e stands for outside surrounding medium. The fluid jet is a charged conductor with dielectric constant ε_i, characterized by zero field inside, surface potential ψ_s and charge σ_s whereas the outside medium is a perfect dielectric with dielectric constant ε_e. The jet is subjected to radial electric field of strength E_0.

A. Governing Equations

The governing equations of motion for the system are given by

$$\tilde{\nabla} \cdot \tilde{v}_j = 0 \tag{1}$$

$$\rho\left(\frac{\partial \tilde{v}_j}{\partial \tilde{t}} + \tilde{v}_j \cdot \tilde{\nabla}\tilde{v}_j\right) = -\tilde{\nabla}\tilde{p}_j + \mu_j \tilde{\nabla}^2 \tilde{v}_j + \tilde{\rho}_{cj}\tilde{E}_j \tag{2}$$

where j is set as i for the inner fluid and e for the outside fluid. E is the electric field; v is the velocity field, p the pressure, ρ_{cj} is the free charge density and ρ is the fluid density in the bulk. The tilde represents dimensional quantities.

In the absence of any free charge i.e. $\rho_c = 0$, the potential (φ) is described by

$$\tilde{\nabla}^2 \tilde{\phi}_j = 0 \tag{3}$$

and $E = -\nabla\phi$

The above governing equations are non-dimensionalized using the following scaling: the distance is scaled by a, the time by $\mu_i a\gamma$, the velocities are scaled by γ/μ_i and the stresses and the pressure by γ/a, where γ represents the interfacial surface tension between the jet and the surrounding fluid. The scaling for potential and electric field are, $\sqrt{\gamma a/(\varepsilon_e \varepsilon_0)}$ and $\sqrt{\gamma/(a\varepsilon_e\varepsilon_0)}$ respectively,

where ε_0 is the permittivity of free space.

Using the above scaling, we get,

$$\nabla \cdot v_j = 0 \tag{4}$$

$$\frac{1}{(Oh_j)^2}\left(\frac{\partial v_j}{\partial t} + v_j \cdot \nabla v_j\right) = -\nabla p_j + c_j \nabla^2 v_j \tag{5}$$

$$\nabla^2 \phi_j = 0 \tag{6}$$

where Oh_j (Ohnesorge number) $= \mu_i/(\rho_j a\gamma)^{1/2}$ and $c_j = \mu_e/\mu_i$ or 1 for the inner jet or outer medium respectively. The viscosity ratio μ_e/μ_i is represented by λ.

In the present work, we specifically look at the case of very high Oh, Stokes flow conditions, which as described in the introduction are common in many industrial processes and biological systems. These conditions are satisfied for flow systems with highly viscous fluid jet and/or for very small diameter cylindrical jets.

Equation 5 is thus reduced to,

$$0 = -\nabla p_j + c_j \nabla^2 v_j \tag{7}$$

B. Boundary Conditions

The electrostatic boundary condition at the interface of the conductor jet and the dielectric surrounding is given by constant potential $\tilde{\phi} = \tilde{\phi}_s$, where the non-dimensional surface potential is given by

$$\phi_i = \phi_o = \psi_s = \tilde{\phi}_s / \left(\sqrt{\tilde{\gamma}\tilde{a}/\varepsilon_0}\right) \tag{8}$$

The hydrodynamic boundary conditions are the continuity of velocity and the force balance at the interface. We use the definitions of the unit normal and the unit tangents to the interface and the velocity vector $v = v_r e_r + v_\theta e_\theta + v_z e_z$ to write the boundary conditions as

$$n \cdot (v_i(r,\theta,z,t) - v_o(r,\theta,z,t)) = 0 \tag{9}$$

$$t_1 \cdot (v_i(r,\theta,z,t) - v_o(r,\theta,z,t)) = 0 \tag{10}$$

$$t_2 \cdot (v_i(r,\theta,z,t) - v_o(r,\theta,z,t)) = 0 \tag{11}$$

$$n \cdot v_i(r,\theta,z,t) - \frac{\partial F(\theta,t)}{\partial t} = 0 \tag{12}$$

$$n \cdot (\tau_i(r,\theta,z,t) + \tau_i^e(r,\theta,z,t) - \tau_o(r,\theta,z,t) - \tau_o^e(r,\theta,z,t)) \cdot n + H(\theta,t) = 0 \tag{13}$$

$$t_1 \cdot (\tau_i(r,\theta,z,t) + \tau_i^e(r,\theta,z,t) - \tau_o(r,\theta,z,t) - \tau_o^e(r,\theta,z,t)) \cdot n = 0 \tag{14}$$

$$t_2 \cdot (\tau_i(r,\theta,z,t) + \tau_i^e(r,\theta,z,t) - \tau_o(r,\theta,z,t) - \tau_o^e(r,\theta,z,t)) \cdot n = 0 \tag{15}$$

where, n, is the unit normal and t_1 and t_2 are the mutually orthogonal unit tangent vectors respectively.

C. Linear Stability Analysis (LSA)

In LSA a typical variable f is expressed as,

$$f = f_m + \delta f' \tag{16}$$

where f_m is the base state (steady state value) and f' is the perturbation variable δ being a small parameter. The analysis is conducted to O(δ).

The perturbed quantity f' is

$$f' = f(r)\int ds \int dk \int dm\ e^{i(kz+m\theta)+st},$$

k and m are the non-dimensional axial and azimuthal wavenumbers and s is the dimensionless growth rate.

The perturbed shape of the interface is given by

$$F(\theta,t) = 1 + \delta D\ e^{i(kz+m\theta)+st} \tag{17}$$

where 1 is the non-dimensional cylinder radius and D is a constant.

The curvature at the perturbed interface is given by

$$H = 1 - \delta D(1 - m^2 - k^2)\ e^{i(kz+m\theta)+st} \tag{18}$$

where the mean curvature of the cylinder is given by 1. Similarly all the other quantities, such as the pressure p, velocity components (v_r, v_θ, v_z) and the potential φ for both inside and outside fluid are decomposed into a base part and a perturbation part. These quantities when substituted back into the governing equations provide eigen functions for the different perturbations variables.

The complete Eigen functions for the potential are directly

obtained by using potential boundary conditions,

$$\phi_i = \psi_s \tag{19}$$

$$\phi_e = \psi_s - E_0 \ln r + \delta \frac{E_0 D}{K_m(k)} K_m(kr)\, e^{i(kz+m\theta)+st} \tag{20}$$

The boundary conditions are applied at the unknown interface F(θ,t) and the value of a typical variable f is obtained from the unperturbed interface as

$$f_{(r=1+D)} = f_{(r=1)} + \left(\frac{\partial f_t}{\partial r}\right)_{r=1} \delta D\, e^{i(kz+m\theta)+st}$$

Substituting the eigen functions in the boundary conditions, one can assemble all the equations in a matrix form as MX=0 where matrix M would be a function of s, k, m, E and λ, and X would be a column matrix made up of all the constants. The matrix equation MX= 0 has a non-trivial solution only when the Det[M] = 0. Solving the determinant of M and equating it to zero gives the dispersion relation, azimuthal wavenumbers along with other operating parameters. The dispersion relation is fairly long and complicated and hence is not shown here. The different elements of the matrix 'X' are provided in the Appendix.

III. Results and Discussion

A. Validation

To validate our problem formulation and solution procedure, we first compare our results with relevant expressions that have been previously reported in the literature for specific values of viscosity ratios, λ.

1) Without Electric Field

Firstly, results of the model without the presence of any electric field are presented. Provide below are the expressions of growth rate for axisymmetric (m = 0) mode for the special case of viscosity ratio λ = 0, 1 and ∞. These three viscosity ratios correspond to a non-viscous vacuum surrounding, similar viscosity fluids and a non-viscous jet respectively.

$$\lambda = 0, \qquad s = \frac{[k^2-1]/2}{(1+k^2-k^2\frac{K_0(k)^2}{K_1(k)^2})} \tag{21}$$

$$\lambda = \infty, \qquad s = \frac{[1-k^2]/2}{(1+k^2-k^2\frac{K_0(k)^2}{K_1(k)^2})} \tag{22}$$

$$\lambda = 1, \qquad s = \frac{k[1-k^2]}{2}(I_1(k)K_2(k) - I_0(k)K_1(k)) \tag{23}$$

Equations (21), (22) and (23) agree with that derived previously under same conditions by Rayleigh [36], Tomotika [37] and Stone and Brenner [38] respectively. Similar to axisymmetric mode, the growth rate expression for the asymmetric m = 1 mode was derived. As previously observed [39]–[41], the asymmetric mode was found to be stable (-ve growth rate) for all values of k, at zero electric field. For m = 1 mode, the growth rate expression for a jet in a non-viscous medium (λ → 0) is,

$$s = \frac{(k\gamma(-2k^2+k(5+k^2)c-2(1+k^2)c^2+2kc^3)}{2(-2k^3+k^2(9+k^2)c-12kc^2-(-4+k^4+4k^2)c^3)} \tag{24}$$

where c = I_1 (k)/I_0 (k).

2) With Radial Electric Field

The expressions of growth rate for axisymmetric and asymmetric perturbations on a viscous conducting jet, in an immiscible viscous dielectric surrounding, subjected to radial electric fields are derived. For the limiting case of λ → 0, a low k analysis was performed for both m = 0 and m = 1 mode. The expressions obtained are,

$$s \sim \frac{1}{6}[\gamma - \varepsilon_e E_{oR}^2], \qquad m = 0 \tag{25}$$

$$s \sim \frac{4}{3k^2}[1 + \varepsilon_e E_{oR}^2 \ln(k)], \qquad m = 1 \tag{26}$$

Equations (25) and (26) agree with the expressions derived by Saville [16] under similar conditions. Radial electric field is known to have a dual effect on axisymmetric perturbations, stabilizing the long waves while destabilizing the short ones.

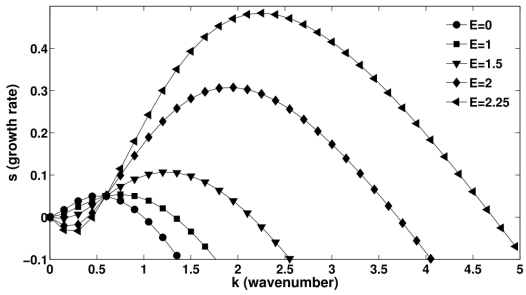

Fig. 1 Effect of radial electric field on m = 0 mode at λ=0.5

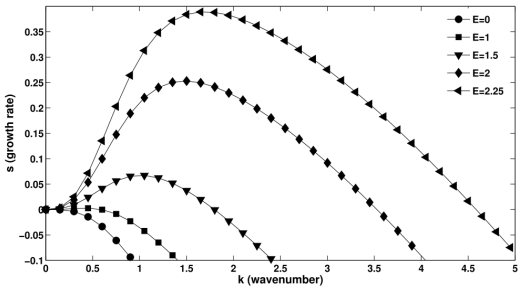

Fig. 2 Effect of radial electric field on m = 1 mode at λ=0.5

On the other hand, asymmetric perturbations have been shown to become more unstable with increasing radial field for all wavelengths. The results obtained in the present work agree with previous investigations as shown in figures 1 and 2.

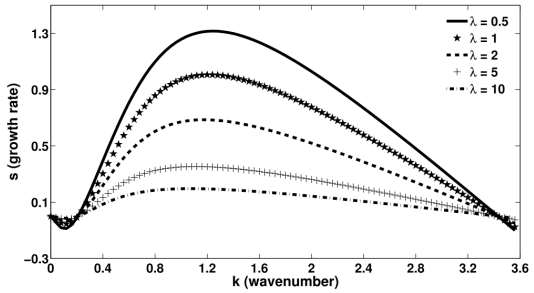

Fig. 3 Effect of λ on m = 0 mode at $E_0 = 3$

With the scaling used in the present work, for the radial electric field orientation the normal and tangential electric stresses do not depend upon the dielectric constant ratio, $\beta = \varepsilon_e / \varepsilon_i$

B. Effect of Viscosity Ratio in Presence of Radial Electric Field

The effect of viscosity ratio λ on liquid-liquid jets when subjected to radial electric field is now discussed. The analysis is restricted to m = 0 and m = 1 mode of perturbation.

Figures 3 and 4 show the growth rate vs wavenumber plots at different λ for m = 0 and m = 1 mode respectively whereas fig. 5 shows the variation of maximum growth rate (s_m) with λ at $E_0 = 3$. Figures 3 and 4 suggest stabilization of both axisymmetric and asymmetric instability with increase in λ. The maximum growth rate, s_m for both m = 0 and m = 1 mode decreases with λ (Fig. 5).

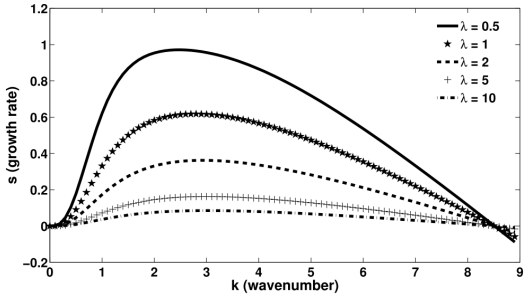

Fig. 4 Effect of λ on m = 1 mode at $E_0 = 3$

Thus it is seen that electric field and viscosity ratio have opposing actions on the growth rates of the two modes of instabilities. Radial electric field on one hand destabilizes whereas viscosity ratio on the other stabilizes these perturbations.

Additionally, the extent with which both these parameters act is different for the two modes. Thus it is very important to study the effect of electric field and viscosity ratio simultaneously. To this end, an operating diagram showing domains of predominance of the two modes for any given value of E 0 and λ is presented in fig. 6.

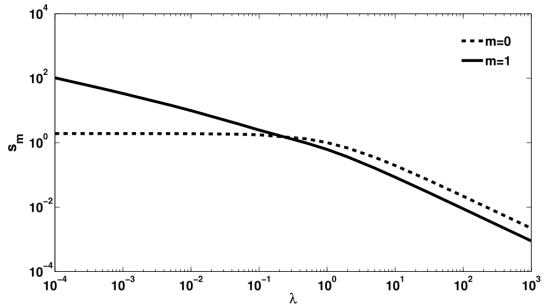

Fig. 5 Effect of λ on s_m for m = 0 and m = 1 mode at $E_0 = 3$

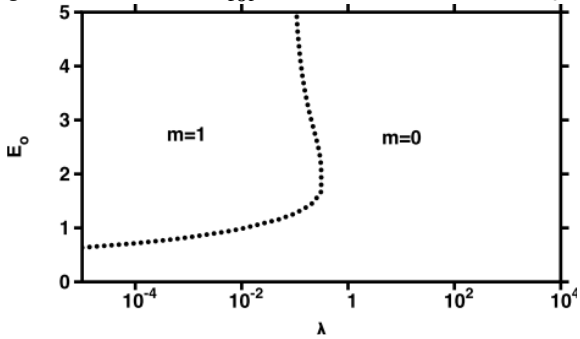

Fig. 6 Operating diagram showing domains of pre-dominance of m = 0 and m = 1 modes for radial electric field

Fig. 6 shows that the m = 1 mode can only be realized in the lower λ limit. Also, at λ values where m = 1 mode dominates, a minimum threshold electric potential must be provided to overcome the axisymmetric m = 0 mode. With increasing λ this threshold electric field also increases, however, this rule is only valid up to a certain critical λ above which the m = 0 mode is always dominant.

IV. Conclusion

The current study presents the linear stability analysis on a fluid jet immersed in another immiscible fluid and subjected to radial electric field. The analysis reduces to the previously reported results for axisymmetric perturbations in the appropriate limits of the viscosity ratio and extends to include asymmetric perturbations along with the effect of changing viscosity ratio and applied electric field. While the effects of electric field on fluid jets are already known, it is found that even the viscosity ratio of the fluids was critically important in deciding the most dominant mode of perturbation.

Increasing λ has a tendency to damp both axisymmetric (m=0) and asymmetric (m=1) modes of instabilities, however the effect is more pronounced for m = 1 mode as compared to m = 0 mode. Thus as λ goes up, the threshold electric field required to express m = 1 mode also rises. An operating diagram to predict the pre-dominant mode at any given value of electric field and viscosity ratio is presented. This diagram can be of great help in correctly predicting the operating conditions required to express any desired instability for a particular application.

APPENDIX

ELEMENTS OF THE MATRIX M

$$\mathbf{M11} = \frac{1}{8}(I_{-2+m}(k) + 2I_m(k) + I_{2+m}(k))$$
$$\mathbf{M12} = I_{-1+m}(k),$$
$$\mathbf{M13} = I_{1+m}(k),$$
$$\mathbf{M14} = \frac{1}{8}(-K_{-2+m}(k) - 2K_m(k) - K_{2+m}(k)),$$
$$\mathbf{M15} = -K_{-1+m}(k),$$
$$\mathbf{M16} = -K_{1+m}(k),$$
$$\mathbf{M17} = 0,$$
$$\mathbf{M21} = \frac{1}{8}i(I_{-2+m}(k) - I_{2+m}(k)),$$
$$\mathbf{M22} = iI_{-1+m}(k),$$
$$\mathbf{M22} = -iI_{1+m}(k),$$
$$\mathbf{M24} = \frac{1}{8}i(-K_{-2+m}(k) + K_{2+m}(k)),$$
$$\mathbf{M25} = -iK_{-1+m}(k),$$
$$\mathbf{M26} = iK_{1+m}(k),$$
$$\mathbf{M27} = 0,$$
$$\mathbf{M31} = \frac{1}{8}(I_{-2+m}(k) + 2I_m(k)) + I_{2+m}(k))$$
$$\mathbf{M32} = I_{-1+m}(k),$$
$$\mathbf{M33} = I_{1+m}(k)$$
$$\mathbf{M34} = 0,$$
$$\mathbf{M35} = 0,$$
$$\mathbf{M36} = 0,$$
$$\mathbf{M37} = -s$$
$$\mathbf{M41} = \frac{1}{8}(kI_{-3+m}(k) + 2I_{-2+m}(k) + 3kI_{-1+m}(k) - 4I_m(k) + 3kI_{1+m}(k) + 2I_{2+m}(k) + kI_{3+m}(k))$$
$$\mathbf{M42} = k(I_{-2+m}(k) + I_m(k)),$$
$$\mathbf{M43} = k(I_m(k) + I_{2+m}(k)),$$
$$\mathbf{M44} = \frac{1}{8}\lambda(kK_{-3+m}(k) - 2K_{-2+m}(k) + 3kK_{-1+m}(k) + 4K_m(k) + 3kK_{1+m}(k) - 2K_{2+m}(k) + kK_{3+m}(k)$$
$$\mathbf{M45} = k\lambda(K_{-2+m}(k) + K_m(k)),$$
$$\mathbf{M46} = k\lambda(K_{-2+m}(k) + K_m(k)),$$
$$\mathbf{M47} = -Eo^2\, k\, K_{-1+m}(k) - 2(E_0^2 + (-1 + k^2 + m^2)\,\gamma)\, K_m(k) + E_0^2\, k\, K_{1+m}(k)\, 2\, K_m(k)$$
$$\mathbf{M51} = \frac{1}{16}i(kI_{-3+m}(k) + 2mI_{-2+m}(k) + kI_{-1+m}(k) + 4\,m\,I_m(k) - kI_{1+m}(k) + 2mI_{2+m}(k) - kI_{3+m}(k))$$
$$\mathbf{M52} = \frac{1}{2}i(kI_{-2+m}(k) + 2(-1 + m)I_{-1+m}(k) + kI_m(k))$$
$$\mathbf{M53} = -\frac{1}{2}i(kI_m(k) - 2(1 + m)I_{1+m}(k) + kI_{2+m}(k)$$
$$\mathbf{M54} = \frac{1}{16}i\lambda(k\,K_{-3+m}(k) - 2\,m\,K_{-2+m}(k) + k\,K_{-1+m}(k) + 4\,m\,K_m(k) - k\,K_{1+m}(k) - 2\,m\,K_{2+m}(k) - k\,K_{3+m}(k))$$
$$\mathbf{M55} = \frac{1}{2}i\lambda(k\,K_{-2+m}(k) - 2(-1 + m)\,K_{-1+m}(k) + k\,K_m(k))$$
$$\mathbf{M56} = -\frac{1}{2}i\lambda(k\,K_m(k) + 2(1 + m)\,K_{1+m}(k) + k\,K_{2+m}(k))$$
$$\mathbf{M57} = 0,$$

$$\mathbf{M61} = \frac{i}{4k}(kI_{-1+m}(k) + 2I_m(k)) + kI_{1+m}(k),$$
$$\mathbf{M62} = iI_m(k)$$
$$\mathbf{M63} = iI_m(k),$$
$$\mathbf{M64} = \frac{1}{4k}(i(kK_{-1+m}(k) - 2K_m(k) + kK_{1+m}(k))$$
$$\mathbf{M65} = iK_m(k),$$
$$\mathbf{M66} = iK_m(k),$$
$$\mathbf{M67} = 0$$

$$\mathbf{M71} = -\frac{1}{8}i(k(-2 + \lambda)I_{-2+m}(k) - 4I_{-1+m}(k) - 4kI_m(k) + 2k\lambda I_m(k) - 4I_{1+m}(k) - 2kI_{2+m}(k) + k\lambda I_{2+m}(k))$$
$$\mathbf{M72} = -\frac{1}{2}ik((-3 + 2\lambda)I_{-1+m}(k) - I_{1+m}(k))$$
$$\mathbf{M73} = \frac{1}{2}i\,k\,(I_{-1+m}(k) + (3 - 2\lambda)I_{1+m}(k))$$
$$\mathbf{M74} = -\frac{1}{8}i\lambda(k\,K_{-2+m}(k) - 4K_{-1+m}(k) + 2k\,K_m(k) - 4\,K_{1+m}(k) + k\,K_{2+m}(k)$$
$$\mathbf{M75} = -\frac{1}{2}ik\lambda(K_{-1+m}(k) + K_{1+m}(k)),$$
$$\mathbf{M76} = -\frac{1}{2}ik\lambda(K_{-1+m}(k) + K_{1+m}(k))$$
$$\mathbf{M77} = 0$$

ACKNOWLEDGMENT

The authors are thankful to P. Sunthar, Prabhakar Ranganathan and Ravi Prakash Jagadeeshan for all the useful discussions. They would also like to thank Leslie Yeo for his detailed comments and criticism on this work.

REFERENCES

[1] C Tsouris, S H Neal, V M Shah, M A Spurrier, and M K Lee. Comparison of Liquid-Liquid Dispersions Formed by a Stirred. Tank and Electrostatic Spraying. Chem. Eng. Commun., 160(1):175–197, jun 1997.

[2] M Sato, T Hatori, and M Saito. Experimental investigation of droplet formation mechanisms by electrostatic dispersion in a liquidliquid system. IEEE Trans. Ind. Appl., 33(6), 1997.

[3] C Tsouris and WT Shin. Pumping, spraying, and mixing of fluids by electric fields. Can. J. Chem. Eng., 76:589–599, 1998.

[4] A Barrero, JM Lopez-Herrera, A Boucard, IG Loscertales, and M Marquez. Steady cone-jet electrosprays in liquid insulator baths. J. Colloid Interface Sci., 272(1):104–108, 2004.

[5] S.N. Jayasinghe. Submerged electrosprays : A versatile approach for microencapsulation. J. Microencapsul., 24:430–444, 2007.

[6] A.G. Marin, I.G. Loscertales, and A. Barrero. Conical tips inside cone-jet electrosprays. Phys. Fluids, 20:042102, 2008.

[7] Guillaume Riboux, ´Alvaro G Mar´ın, Ignacio G Loscertales, and Antonio Barrero. Whipping instability characterization of an electrified visco-capillary jet. J. Fluid Mech., 671:226–253, 2011.

[8] MS Alexander. Pulsating electrospray modes at the liquid-liquid interface. Appl. Phys. Lett., 92(14):144102, 2009.

[9] Jens Eggers. Nonlinear dynamics and breakup of free-surface flows. Rev. Mod. Phys., 3:865–929, 1997.

[10] R. D. Lin, S. P.and Reitz. Drop and spray formation from a liquid jet. Ann. Rev. Fluid Mech., 30:85–105, 1998.

[11] J. Eggers and E. Villermaux. Nonlinear dynamics and breakup of free-surface flows. Rev. Mod. Phys., 71:036601, 2008.

[12] AL Huebner and HN Chu. Instability and breakup of charged liquid jets. J. Fluid Mech., 49:361–372, 1971.

[13] G Artana, H Romat, and G Touchard. Theoretical analysis of linear stability of electrified jets flowing at high velocity inside a coaxial electrode. J. Electrostat., 43(2):83–100, 1998.

[14] EK Elcoot. Nonlinear instability of charged liquid jets: Effect of interfacial charge relaxation. Physica A, 375(2):411–428, 2007.

[15] AB Basset. Waves and jets in a viscous liquid. Am. J. Math., 16(1):9 110, 1894.

[16] DA Saville. Stability of electrically charged viscous cylinders. Phys. Fluids, 14:1095–1099, 1971b.

[17] RJ Turnbull. On the instability of an electrostatically sprayed liquid jet. IEEE Trans. Ind. Appl., 28(6):1432–1438, 1992.

[18] RPA Hartman, DJ Brunner, DMA Camelot, JCM Marijnissen, and B Scarlett. Jet break-up in electrohydrodynamic atomization in the cone-jet mode. J. Aerosol Sci. 31(1):65–95, 2000.

[19] H Gonz´alez, FJ Garc´ıa, and A Castellanos. Stability analysis of conducting jets under ac radial electric fields for arbitrary viscosity. Phys. Fluids, 15:395–407, 2003.

[20] JM L´opez-Herrera and AM Ganan-Calvo. A note on charged capillary jet breakup of conducting liquids: experimental validation of a viscous one-dimensional model. J. Fluid Mech., 501:303–326, 2004.
[21] JM L´opez-Herrera, P Riesco-Chueca, and AM Ga˜n´an-Calvo. Linear stability analysis of axisymmetric perturbations in imperfectly conducting liquid jets. Phys. Fluids, 17:034106, 2005.
[22] FJ Higuera. Stationary viscosity-dominated electrified capillary jets. J. Fluid Mech., 558:143–452, 2006.
[23] RT Collins, MT Harris, and OA Basaran. Breakup of electrified jets. J. Fluid Mech., 588:75–129, 2007.
[24] Qiming Wang, S M¨ahlmann, and D T Papageorgiou. Dynamics of liquid jets and threads under the action of radial electric fields: Microthread formation and touchdown singularities. Phys. Fluids, 21(3):032109, 2009.
[25] D T Conroy, O K Matar, R V Craster, and D T Papageorgiou. Breakup of an electrified viscous thread with charged surfactants. Phys. Fluids, 23(2):022103, 2011.
[26] FJ Higuera. Stationary coaxial electrified jet of a dielectric liquid surrounded by a conductive liquid. Phys. Fluids, 19:012102, 2007.
[27] FJ Higuera. Electrodispersion of a liquid of finite electrical conductivity in an immiscible dielectric liquid. Phys. Fluids, 22:112107, 2010.
[28] Li Fang, Yin Xie-Yuan, and Yin Xie-zhen. Instability of a leaky dielectric coaxial jet in both axial and radial electric fields. Phys. Rev. E, 78:036302, 2008.
[29] Li Fang, Yin Xie-Yuan, and Yin Xie-zhen. Instability of a viscous coflowing jet in a radial electric field. J. Fluid Mech., 596:285–311, 2008.
[30] Li Fang, Yin Xie-Yuan, and Yin Xie-zhen. Axisymmetric and non-axisymmetric instability of an electrified viscous coaxial jet. J. Fluid Mech., 632:199–225, 2009.
[31] MN Reddy and A Esmaeeli. The EHD-driven fluid flow and deformation of a liquid jet by a transverse electric field. Int. J. Multiphase Flow, 35(11):1051–1065, 2009.
[32] H Gonz´alez and FMJ McCluskey. Stabilization of dielectric liquid bridges by electric fields in the absence of gravity. J. Fluid Mech., 206:545–561, 1989.
[33] MJ Marr-Lyon, DB Thiessen, and FJ Blonigen. Stabilization of electrically conducting capillary bridges using feedback control of radial electrostatic stresses and the shapes of extended bridges. Phys. Fluids, 12:986–995, 2000.
[34] C L Burcham and D A Saville. Electrohydrodynamic stability: Taylor–Melcher theory for a liquid bridge suspended in a dielectric gas. J. Fluid Mech., 452:1–25, feb 2002.
[35] A Onuki. Electric field effects near critical points. In SJ Rzoska and VP Zhelezny, editors, Nonlinear Dielectric Phenomena in Complex Liquids, Vol. 157. NATO Science Series, 2005.
[36] L Rayleigh. On the instability of a cylinder of viscous liquid under capillary force. Phil. Mag., 34:145–154, 1892.
[37] S Tomotika. On the instability of a cylindrical thread of a viscous liquid surrounded by another viscous fluid. Proc. Roy. Soc. London A, 150:322–337, 1935.
[38] HA Stone and MP Brenner. Note on the capillary thread instability for fluids of equal viscosities. J. Fluid Mech., 318:373–374, 1996.
[39] DA Saville. Electrohydrodynamic stability: effects of charge relaxation at the interface of a liquid jet. J. Fluid Mech., 48(04):815–827, 1971.
[40] AJ Mestel. Electrohydrodynamic stability of a highly viscous jet. J. Fluid Mech., 312:311–326, 1996.
[41] PH Son and K Ohba. Theoretical and experimental investigations on instability of an electrically charged liquid jet. Int. J. Multiphase Flow, 24(4):605–615, 1998.